3D imaging, visualization, and recognition of biological microorganisms

Bahram Javidi, Inkyu Moon and Mehdi Daneshpanah
Dept. of Electrical and Computer Engineering, U-2157, University of Connecticut,
Storrs, CT USA 06269-2157

ABSTRACT

In this paper, we address coherent optical imaging techniques for real time automated three-dimensional (3D) sensing, visualization and recognition of dynamic biological microorganisms. Real time sensing and 3D reconstruction of the dynamic biological microorganisms is performed using the single-exposure on-line (SEOL) digital holographic microscopy. A coherent 3D microscope-based interferometer is used to record digital holograms of dynamic micro biological events. Complex amplitude 3D images of the biological microorganisms are computationally reconstructed at different depths by Fresnel propagation algorithm. Statistical segmentation algorithms are applied to identify regions of interest for further processing. Statistical pattern recognition approaches are addressed to identify and recognize the microorganisms. Experimental results with biological microorganisms are presented to illustrate detection, segmentation, and identification of biological events.

Keywords: digital holography, pattern recognition and 3D image processing

1. INTRODUCTION

Optical coherent imaging systems by digital holography have been studied for three-dimensional (3D) visualization and recognition of objects. Digital holographic-based 3D microscopy has been applied to the 3D sensing, visualization and recognition of microorganisms [1-4]. It automatically produces focused images of biological microorganisms from only one digital hologram without any mechanical scanning which is necessary in conventional microscopy. Also, the depth information of the biological microorganisms can be obtained by analyzing coherent interference pattern. The single-exposure on-line (SEOL) digital holography enables one to three-dimensionally sense, monitor and recognize the moving, growing and reproducing biological cells. The SEOL digital holographic microscopy allows computationally reconstructed 3D imaging of the growing and dividing biological cells from only one digital hologram. A single hologram provides a snapshot, thus it doesn't have the dynamic information.

In particular, study of harmful biological microorganisms or other biological cells has many potential applications in national security and defense or new medical treatments. Recently, public health officials have concerned about an avian flu virus that could be the next pandemic in the world. It has been reported that an avian flu virus could be the next pandemic. Therefore, the development of reliable, automated, and low-cost methods for real time detection and identification of harmful bacteria and viruses are of significant benefits and essential in combating catastrophic diseases. However, Conventional methods in practice for inspecting most bacteria or viruses involve bio-chemical processing which are not real-time and very time-consuming.

Real-time automatic recognition of living organisms is a very difficult task for a number of reasons. Biological microorganisms are dynamic events and not rigid objects. They can move, grow, and reproduce themselves, and vary in size and shape among the same species. In particular, bacteria and viruses are very small and simple morphological traits. They may occur as a single cell or form an association of various complexities according to the environmental conditions. Conventional methods in this field have been aimed to recognize cells through bio-chemical analyses. Most image-based recognition efforts for specific microorganisms have been based on two-dimensional (2D) intensity images which may not be effective.

In this report, we present a new 3D sensing and recognition system of biological microorganisms using the optical coherent 3D imaging based on digital holographic microscopy, digital imaging processing methods.

Three-Dimensional TV, Video, and Display V, edited by Bahram Javidi, Fumio Okano, Jung-Young Son
Proc. of SPIE Vol. 6392, 639202, (2006) · 0277-786X/06/$15 · doi: 10.1117/12.694417

The Fresnel diffraction patterns of biological microorganisms are optically recorded by SEOL holographic microscopy. Then, the complex magnitude 3D images of the biological microorganisms are numerically reconstructed from the SEOL digital hologram. For the 3D recognition, Segmentation of the reconstructed 3D images of microorganisms can be accomplished using bivariate jointly distributed region snakes method. Conventional segmentation techniques based on the edge map may fail to segment these images appropriately. We present a statistical framework based on the joint probability distribution of magnitude and phase information of SEOL holographic microscopy images and maximum likelihood estimation of parameters for the joint probability density function. An optimization criterion is computed by maximizing the likelihood function of the target support hypothesis. After the segmentation the recognition of microorganisms can be performed by analyzing the 3D complex morphology of the computationally reconstructed holographic images. A number of sampling segments are randomly extracted from the reconstructed 3D image of microorganisms. By selecting arbitrary sampling segments and testing them through statistical inference, we can develop a recognition system which is independent of the shape of microorganisms.

Fig. 1 shows the frameworks and design procedure for the 3D sensing and recognition based on SEOL holographic microscopy. The following sections describe various stages of the proposed approach for 3D sensing and recognition of biological microorganisms by use of optical coherent imaging based on digital holographic microscopy. In chapter 1, we briefly describe the concept of SEOL digital holographic microscopy. The segmentation of the complex-valued biological microorganism images using the regional segmentation method is presented in chapter 2. Microorganism recognition using 3D complex morphology of the reconstructed images is presented in chapter 3. Finally, the conclusion follows.

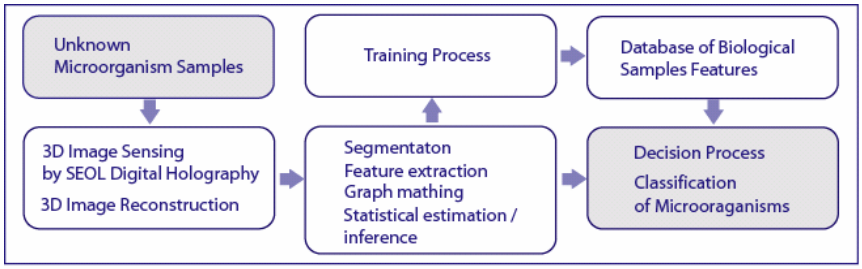

Fig. 1. Frameworks for 3D sensing, visualization and recognition of biological microorganisms using SEOL holographic microscopy.

2. DIGIAL HOLOGRAPHIC MICROSCOPY

In the following, The SEOL digital hologram of biological microorganisms in the Fresnel domain is recorded by the CCD (Charge-Coupled Device) array using reference plane wave as shown in Fig 2 [1-4]. An Argon laser (center wavelength of 514.5 nm) as a light source is used for a spatial and temporal coherence imaging. The coherence light source illuminates the specimen and then it is magnified by the microscope objective. The focused image at the image plane starts to diffract. The interference intensity pattern is generated by the plane-parallel reference wave and the diffracted wave-fronts of the specimen.

Our system requires that only a single exposure is recorded for obtaining Fresnel diffracted intensity pattern of a stem cell, therefore the SEOL digital holographic microscopy can be suitable for recognizing and identifying a growing and dividing stem cell and robust to a external noise factor such as fluctuation and vibration. The field distribution of stem cells at the CCD plane or hologram plane is represented as follows:

$$O_H(x,y) = A_{OH}(x,y)e^{j\phi_{OH}(x,y)} = \iint\int_{d_0-\frac{\delta}{2}}^{d_0+\frac{\delta}{2}} \left\{ \frac{e^{j2\pi z/\lambda}}{j\lambda z} e^{j\frac{\pi}{\lambda z}(x^2+y^2)} O(\xi,\eta;z) e^{j\frac{\pi}{\lambda z}(\xi^2+\eta^2)} e^{-j\frac{2\pi}{\lambda z}(x\xi+y\eta)} \right\} dz d\xi d\eta \,, \tag{1}$$

where $O(\xi,\eta;z)$ is the field distribution of original biological microorganism at the image plane, d_0 is the distance between the center of the focused biological microorganism at the image plane and hologram plane and δ is the cell's depth along z-axis. The interference intensity pattern or the SEOL digital hologram between diffracted wave-fronts of

biological microorganism and plane parallel reference wave recorded at the CCD plane or hologram plane is represented as follow:

$$H(x,y) = A_{OH}(x,y)^2 + A_R^2 + 2A_{OH}(x,y)A_R \cos[\phi_{OH}(x,y) - \phi_R], \tag{2}$$

where $A_R e^{j\phi_R}$ is the reference wave at the hologram plane. The 3D reconstruction of the original biological microorganism is performed computationally by using inverse Fresnel transformation from the SEOL digital hologram. Finally, the field distribution of the reconstructed 3D biological microorganism from SEOL digital hologram can be represented as follows:

$$\hat{O}(\xi,\eta) = IFrT\left(FrT\{H(x,y)\} \times \exp\{j\pi\lambda d_o[\frac{u^2}{(\Delta x N_x)^2} + \frac{v^2}{(\Delta y N_y)^2}]\} \right) \tag{3}$$

where d_0 is the distance between the CCD plane (hologram plane) and the image plane, u and v denote transverse discrete spatial frequencies, $(\Delta x, \Delta y)$, and (N_x, N_y) are the size and the number of pixels of the CCD at the hologram plane, respectively, and $FrT\{\cdot\}$ means Fresnel transformation. The reconstructed 3D biological microorganism's image from the SEOL digital hologram originally contains a conjugate image. This undesired component may degrade the quality of the reconstructed 3D image, but the intrinsic defocused conjugate image also contains information of the 3D biological microorganisms. As an additional merit, SEOL digital holography allows us to obtain a dynamic time-varying scene reconstructed digitally on the computer for monitoring and recognizing dividing and growing cells.

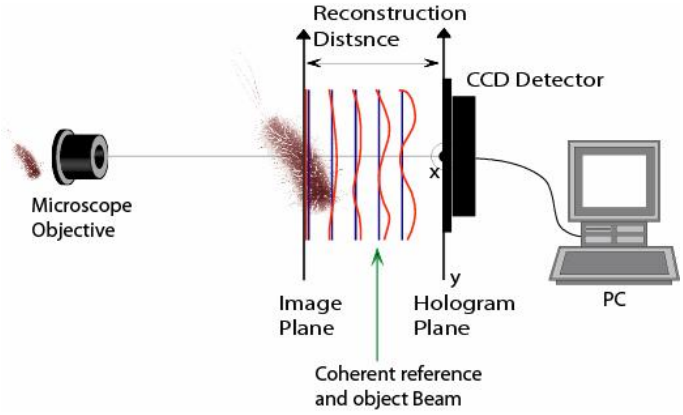

Fig. 2. Schematic setup of the SEOL digital holography for the 3D sensing and recording of biological microorganisms.

3. 3D BIOLOGICAL MICROORGANISM SEGMENTATION

A critical step for microorganism identification is the segmentation of reconstructed images, which can facilitate proper detection and recognition. In this section, we address the segmentation of SEOL holographic images of microorganisms using bivariate jointly distributed region snakes which is based on statistically independent region snakes [4]. This technique is built on a statistical framework capable of handling images with complex-valued pixels and the joint probability distribution of magnitude and phase information of the scene. Within this framework, the optimization criterion is computed by maximizing the likelihood function of the target support hypothesis H_w, while no knowledge of the statistical properties of the target/background is assumed as *a priori*. Instead, a maximum likelihood estimator estimates the necessary statistical parameters. Moreover, target and background pixels are assumed to have independent bivariate Gaussian distribution for their magnitude and phase contents, respectively.

This method uses the concept of snake active contours for separating the target from the background scene by a target support hypothesis. A snake is essentially a closed contour that can be approximated by a multi-node polygon, which

evolves during the segmentation process to minimize a certain criterion known as the snake energy. This contour divides the image into inner and outer regions which are denoted by Ω_t (target) and Ω_b (background), respectively. A stochastic algorithm is utilized to carry out the optimization and guide the deformations of the snake to eventually force the snake contour to converge to the original microorganism boundary.

There are several advantages for using the bivariate jointly distributed region snake algorithm. In fact, the bivariate joint distribution of magnitude and phase information provides a more accurate image model for the reconstructed images of SEOL digital holography since it captures the correlation between each pixel's magnitude and phase content. That is in contrast with independent distribution analysis, which treats the magnitude and phase information as independent random variables and consequently ignores the correlation of these two correlated random variables. In addition, in region snakes regime, the evolution of the snake contour is not dependent of local pixels near the contour edge as in classic snake active contours, but rather, the evolution process is based on the statistical distribution of the complex amplitude inside and outside the snake contour. The latter fact facilitates segmentation of objects even when they are out-of-focus or images with jagged object boundaries.

3.1 Methodology

Computational reconstruction of the SEOL hologram obtained from the interference pattern formed on the CCD involves the inverse Fresnel transform. As a result, the reconstructed holographic images have complex-valued pixels, thus each pixel $s_i = \alpha_i \exp(j\varphi_i)$ is a complex number with α_i and φ_i for its magnitude and phase, respectively. The target and background pixels are assumed to follow two independent bivariate normal distributions. Each distribution has a probability density function which consists of two dependent normal random variables α and φ as for magnitude and phase, respectively. The original bivariate normal probability density function is not separable directly. However, conditioning one of the variables (α) on the second variable (φ), one can obtain the separated form of bivariate normal probability distribution function as follows:

$$f_u(\alpha_i,\varphi_i) = \frac{1}{\sigma_\varphi^u}\Phi\left(\frac{\varphi_i-\mu_\varphi^u}{\sigma_\varphi^u}\right)\times\frac{1}{\sigma_{\alpha|\varphi}^u}\Phi\left(\frac{\alpha_i-\mu_{\alpha|\varphi}^u}{\sigma_{\alpha|\varphi}^u}\right), \tag{4}$$

where $\Phi(x)=(2\pi)^{-1/2}\exp(-x^2/2)$ denotes the standard normal distribution. The script $u\in\{t,b\}$ is used to discriminate the target and background respectively. Also, let parameter vector $\Theta_u=\{\mu_\alpha^u,\mu_\varphi^u,\sigma_\alpha^u,\sigma_\varphi^u,\rho_u\}$ be the distribution parameters of either the target or the background. Since the separation of two random variables in Eq. (4) is made possible by conditioning α on φ, the corresponding conditional mean and variances can be used for α as follows:

$$\mu_{\alpha|\varphi}^u = \mu_\alpha^u + \frac{\rho_u\sigma_\alpha^u(\varphi-\mu_\varphi^u)}{\sigma_\varphi^u},\ \sigma_{\alpha|\varphi}^{u\ 2} = \sigma_\alpha^2(1-\rho_u^2). \tag{5}$$

Let $\mathbf{w}=\{w_i \mid i\in[1,N]\}$ be a binary window model that determines the support of the target such that w_i=1 for the pixels of target and w_i=0 elsewhere, and N is the total number of image pixels. Now the image can be represented as the addition of disjoint target complex pixels (**a**) inside the binary window **w**, and background complex pixels (**b**) outside the window. Thus we adopt the one dimensional representation of the image as: $\mathbf{s}_i = \mathbf{a}_i w_i + \mathbf{b}_i[1-w_i]$.

With these notations the problem of segmentation reduces to finding an optimal choice for **w** that maximizes the hypothesis probability $P[H_{\mathbf{w}} \mid \mathbf{s}]$ (i.e. the most likely window **w** of the target), where $H_{\mathbf{w}}$ represents the hypothesis that **w** is the target support. Using the Bayes rule and considering an equally likely hypothesis scenario, the maximization of *a posteriori* hypothesis probability is analogous to maximizing the conditional probability which is expressed as the likelihood function for $H_{\mathbf{w}}$ as following:

$$\mathbf{P}(\mathbf{s}\mid H_{\mathbf{w}},\Theta) = \prod_{i=1}^{N} f_t(\alpha_i,\varphi_i)\cdot w_i \times \prod_{i=1}^{N} f_b(\alpha_i,\varphi_i)\cdot(1-w_i), \tag{6}$$

where vector $\Theta = \{\Theta_t, \Theta_b\}$ contains all the parameters needed to characterize the bivariate normal distributions of the target and background pixels. Since no prior knowledge of the target and background is assumed, these parameters should be estimated. Thus maximum likelihood estimator has been utilized as following:

$$\begin{aligned}
&\hat{\mu}_\alpha^u = \frac{1}{N_u(\mathbf{w})}\sum_{i\in\Omega_u}\alpha_i, \qquad \hat{\mu}_\varphi^u = \frac{1}{N_u(\mathbf{w})}\sum_{i\in\Omega_u}\varphi_i, \\
&\hat{\sigma}_\alpha^u = \left\{\frac{1}{N_u(\mathbf{w})}\sum_{i\in\Omega_u}(\alpha_i - \mu_\alpha^u)^2\right\}^{\frac{1}{2}}, \quad \hat{\sigma}_\varphi^u = \left\{\frac{1}{N_u(\mathbf{w})}\sum_{i\in\Omega_u}(\varphi_i - \mu_\alpha^u)^2\right\}^{\frac{1}{2}}, \\
&\hat{\rho}_u = \frac{1}{N_u(\mathbf{w})\sigma_\alpha^u\sigma_\varphi^u}\sum_{i\in\Omega_u}(\alpha_i - \mu_\alpha^u)(\varphi_i - \mu_\alpha^u),
\end{aligned} \tag{7}$$

where $N_u(\mathbf{w})$ denotes the number of pixels in the target or background window according to the script *u*. By substituting the bivariate joint probability distribution function in Eq. (4) into Eq. (6) and using Eqs. (5) and (7), one can see that maximization of Eq. (6) is analogous to minimization of the following criterion:

$$\mathbf{J}(\mathbf{s} \mid H_\mathbf{w}, \Theta) = N_t(\mathbf{w})\log\left(\hat{\sigma}_\varphi^t\hat{\sigma}_\alpha^t\sqrt{1-\hat{\rho}_t^2}\right) + N_b(\mathbf{w})\log\left(\hat{\sigma}_\varphi^b\hat{\sigma}_\alpha^b\sqrt{1-\hat{\rho}_b^2}\right) \tag{8}$$

Minimization of Eq. (8) leads to maximization of the likelihood function in Eq. (6), thus, this optimization forces the snake polygon (representing $H_\mathbf{w}$) to evolve in such a way to find the statistically optimal $H_\mathbf{w}$ for the target support.

3.2 Stochastic optimization algorithm

In order to carry out the optimization, a simple stochastic algorithm is employed. The basic idea is to model the snake by a polygon with *l* constant points and iteratively deform the polygon nodes in such a way that the optimization criterion in Eq. (8) decreases at every iteration. This procedure is illustrated in the following diagram:

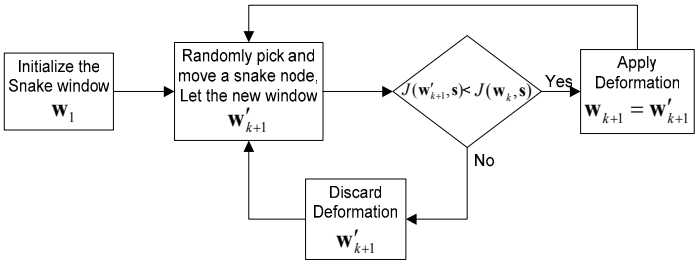

Fig. 3. Schematic diagram of the primary stochastic minimization algorithm.

Several techniques such as multi-resolution snake, adaptive node selection and direction inertia are presented in [46] to increase the robustness and convergence speed of the above algorithm. The algorithm is terminated when no more contraction can be imposed on $\boldsymbol{J}(s,w)$ for long consecutive iterations.

4. SHAPE-INDEPENDENT 3D RECOGNITION APPROACH

We apply statistical algorithms to the 3D recognition system to make it independent of the shape and profile of the microorganisms [2]. The shape-independent recognition approach may be suitable for recognizing 3D microorganisms such as bacteria and biological cells that do not have well defined shapes or profiles. For example, they may be simple, unicellular and branched in their morphological traits. It could also be applied to cells that vary in shape and profile rapidly. For the shape-independent approach, a number of sample segments are randomly extracted from the segmented 3D image of a microorganism. These samples are processed using statistical cost functions to classify the microorganism. The sample distributions for the difference of parameters between the sample segment features of the reference and input images are calculated using statistical estimation.

First, we reconstruct the 3D microorganism as a volume image from a SEOL digital hologram corresponding to a reference microorganism. Then, we randomly extract *N* pixels in the reconstructed 3D image. We repeat the above steps

for *S* specimens of the same class of microorganism. Therefore, each sample segment consists of *N* by *S* complex values. We denote each pixel value in the trial sample patch as $\mathbf{X}_{Nn}^{S}$ [See Fig. 4]. We refer to each reconstruction plane of the 3D volume as "page." Now, we change the locations of each sample in a given page, and repeat the above steps *n* times.

Similarly, we record the SEOL digital hologram of an unknown input microorganism and then restore the original input image. Next, we randomly extract *N* pixels *n* times in the unknown reconstructed 3D image and repeat the above steps about *S* specimens of the same microorganism. Each sample segment consists of *N* by *S* complex values. We have a total of *n* of these segments as well. We denote each pixel value in the trial sample patch as $\mathbf{Y}_{Nn}^{S}$. For classification and recognition of biological microorganisms, we use the statistical inference for the equality of the locations and dispersions between reference sample data and unknown sample data using a statistical sampling and estimation theory.

We assume that random variables $\mathbf{X}_{N}^{S}$ and $\mathbf{Y}_{N}^{S}$ which are elements inside the reference and unknown input sample segment are statistically independent with identical population distribution $f(\mathbf{X})$ and $f(\mathbf{Y})$, respectively. Also, let $\mathbf{X}_{N}^{S}$ be independent of $\mathbf{Y}_{N}^{S}$. It is noted that the reconstructed image from a SEOL hologram consists of complex values, so we perform two separate univariate hypothesis testing about the real part and the imaginary part, respectively.

From the histogram analysis of the real and imaginary parts of the reconstructed 3D images from the SEOL digital hologram, we may consider that the random variables (real or imaginary parts of the reconstructed image) in the sampling segment nearly follow Gaussian distribution. For checking the normality of sample data, the Ch-square goodness of fit test can be performed.

For comparing the variance of two sample segments between reference and input, if the sample data are normally distributed, the following F-test can be used:

$$\mathbf{F}_{(N_{\mathbf{X}}-1),(N_{\mathbf{Y}}-1)} = \frac{\{N_{\mathbf{Y}}/(N_{\mathbf{Y}}-1)\}V[\mathbf{Y}]}{\{N_{\mathbf{X}}/(N_{\mathbf{X}}-1)\}V[\mathbf{X}]} = \frac{\hat{V}[\mathbf{Y}]}{\hat{V}[\mathbf{X}]}, \tag{9}$$

where $N_{\mathbf{X}}$ and $N_{\mathbf{Y}}$ are the number of reference and input sampling segment, respectively; $V[\cdot]$ denotes the variance; and $\hat{V}[\cdot]$ is unbiased sample variance. If the sample data are not normally distributed, we use the following Levene's test by performing an analysis of variance on the absolute deviations of the data from their respective sample:

$$\mathbf{W} = \frac{(N_{\mathbf{X}}+N_{\mathbf{Y}}-2)[N_{\mathbf{X}}(\bar{Z}_{\mathbf{X}}-\bar{Z})^2 + N_{\mathbf{Y}}(\bar{Z}_{\mathbf{Y}}-\bar{Z})^2]}{\sum_{j=1}^{N_{\mathbf{X}}}(Z_{\mathbf{X}j}-\bar{Z}_{\mathbf{X}})^2 + \sum_{j=1}^{N_{\mathbf{Y}}}(Z_{\mathbf{Y}j}-\bar{Z}_{\mathbf{Y}})^2}, \tag{10}$$

where $Z_{\bullet j} = \left|Y_{\bullet j} - \tilde{Y}_{\bullet j}\right|$; $\tilde{Y}_{\bullet j}$ is the sample mean of the reference or unknown input; $\bar{Z}_{\bullet}$ is the sample means of the $Z_{\bullet j}$; and $\bar{Z}$ is the overall mean of the $Z_{\bullet j}$. The sampling segments are extracted in the reconstructed 3D image using SEOL digital hologram.

For comparing the means of two sample segments between reference and input image, if the sample data are normally distributed, the following t-test can be used:

$$\mathbf{T} = \frac{1}{\bar{V}_P}\frac{E[\mathbf{X}]-E[\mathbf{Y}]}{\{(N_{\mathbf{X}})^{-1}+(N_{\mathbf{Y}})^{-1}\}^{1/2}}, \tag{11}$$

where $\bar{V}_P$ is the pooled estimator of the variance of actual population; and $E[\cdot]$ denotes the expectation operator. If the sample data are not normally distributed, we use the following Mann-Whitney test that does not require assumptions about the shape of the underlying distributions by performing an analysis of median from their respective sample:

$$\mathbf{U} = N_{\mathbf{X}}N_{\mathbf{Y}} + \frac{N_{\mathbf{X}}(N_{\mathbf{X}}+1)}{2} - \mathbf{R}_{\mathbf{X}}, \tag{12}$$

where the statistic U is corresponding to the reference image; and $\mathbf{R}_\mathbf{X}$ is the rank sum of the sample data of the reference image. If the sample size is greater than 8, it is known that the statistic U is approximately normally distributed, so Eq. (12) can be $\mathbf{Z} = (\mathbf{U} - \mu_\mathbf{U})/\sigma_\mathbf{U}$, where $\mu_\mathbf{U}$ and $\sigma_\mathbf{U}$ are mean and standard deviation of the statistic U, respectively.

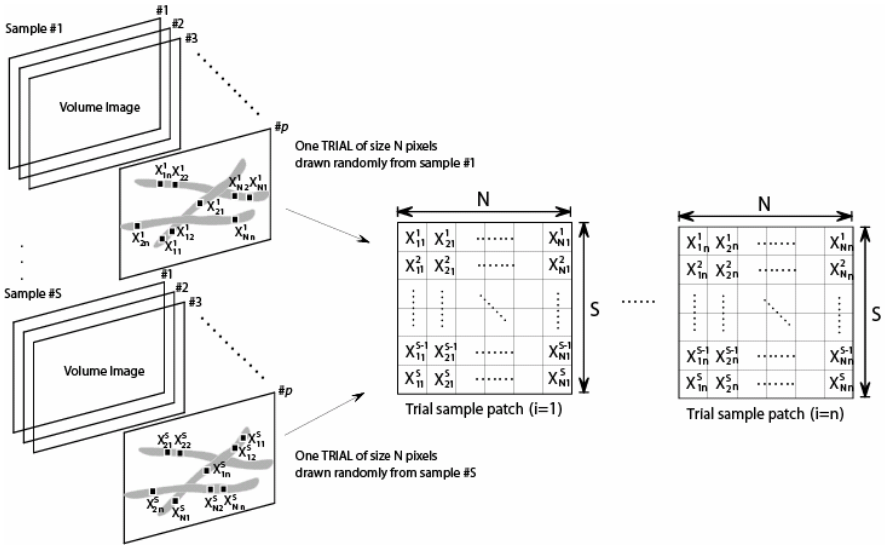

Fig. 4. Design procedure for shape independent 3D recognition of biological microorganisms Recognition.

5. EXPERIMENTAL RESULTS

5.1 Segmentation results

In this section some experimental results of the bivariate region snake segmentation described in Section 3 are presented. Computationally reconstructed images of several microorganisms from SEOL holographic microscopy are used.

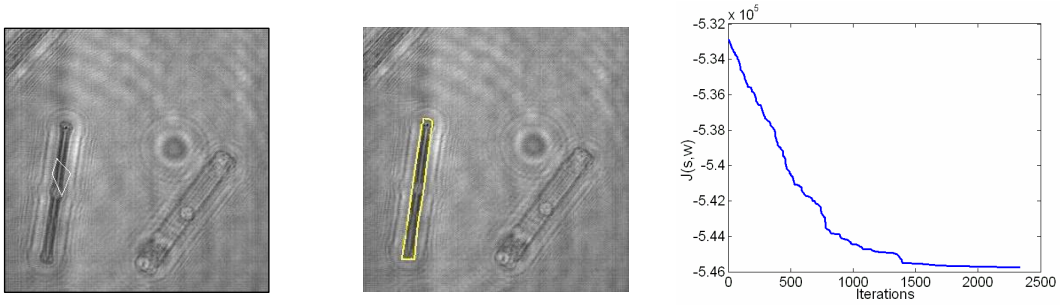

(a) (b) (c)

Fig. 5. (a) Magnitude images of two diatom algae on which the snake is initialized with 4 points, (b) the final segmentation carried out by bivariate region snake after 1500 iterations, (c) the trace of the optimization criterion during the iteration.

As discussed earlier, bivariate jointly distributed region snake incorporates both the magnitude and phase information simultaneously since the holographic images are complex, however, the magnitude images are used for illustration in the figures hereafter. The snake contour is modeled as a polygon with *l* vertexes and the binary window function **w**, is set to 1 inside and 0 outside the polygon. The images in the first column in Fig. 5(a) shows two different diatom algae over which the snakes are initialized with 4 nodes. Although the initial contour is completely different from target boundaries the bivariate region snake is able to capture the microorganism body after approximately 1500 iterations [See Fig. 5(b)]. As it can be seen in Fig. 5(c), the optimization traces obtain a reasonable slope and show very slight progress after the 1500th iteration which can be an indicator to stop the iterations.

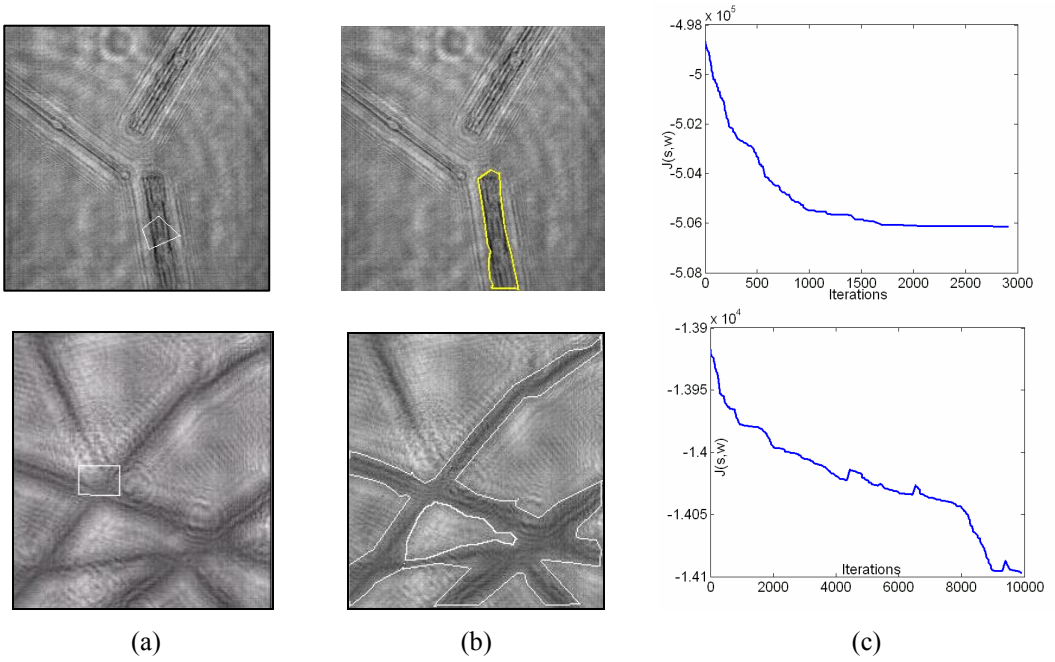

(a) (b) (c)

Fig. 6. (a) Magnitude image of an out-of-focus sphacelaria alga reconstructed from a SEOL hologram and the 5 point snake initialization, (b) the segmented microorganism, (c) the trace of the optimization criterion during the iteration.

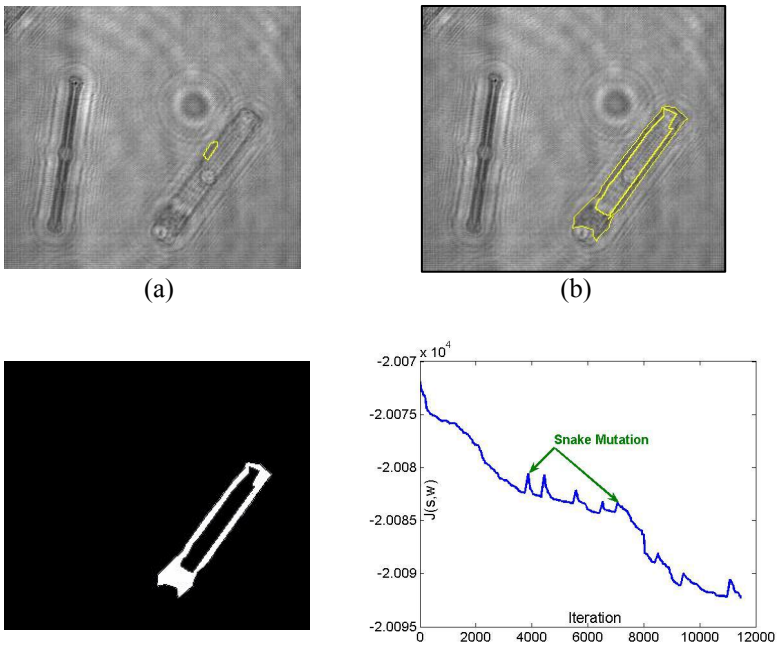

(a) (b)

(c) (d)

Fig. 7. (a) Magnitude image of computationally reconstructed SEOL hologram of diatom algae, (b) segmentation result, (c) the final binary windows w for the target, (d) optimization profile.

In the next example, the segmentation of sphacelaria alga has been illustrated. This alga has a branch-like structure. The initialization captures a small portion of the living organism and throughout the iterations, the snake creeps to capture its whole body. Since the structure of algae requires many snake nodes, and the optimization algorithm's speed is inversely proportional to the number of snake nodes, more iteration is needed to complete the segmentation. Fig. 6(a) is intentionally reconstructed out-of-focus from a SEOL hologram, so it appears blurred without well-defined edges to be more challenging, however, the bivariate region snake shows promising results in Figs. 6(b) and (c).

The next experiment in Fig. 7 shows the segmentation of a diatom, where the boundaries of the microorganism are traced by the snake. The introduction of slight structural mutation on the snake results in small peaks in the optimization profile as shown in Fig. 7(d). These structural mutations are imposed by eliminating unnecessary nodes which lie close to the line segment connecting their previous and next nodes. The optimization plot in Fig. 7(d) shows how mutations can help the snake find its way through narrow passages.

5.2 Experimental results for shape-tolerant 3D microorganism recognition

In this subsection, we conduct statistical estimation and inference to test the performance of our shape tolerant 3D microorganism recognition system using SEOL digital holography. First, 100 trial sampling segment features have been produced by randomly selecting the test pixel points from the segmented oscillatoria bacteria 3D image corresponding to the reference data set, where we changed sample size from 10 to 200. We similarly generated 100 sampling segment features by randomly choosing the test pixel points from the oscillatoria bacteria 3D image as the true-class inputs and in the diatom alga image as the false-class inputs, respectively. The reference and input images are reconstructed at distance d = 270 mm as shown Fig 8.

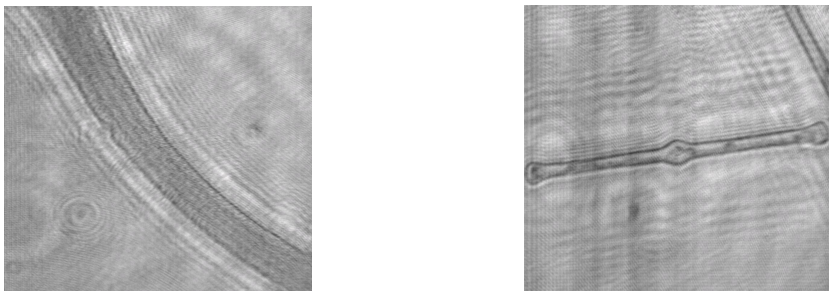

(a) (b)

Fig. 8. The magnified intensity images at the distance d = 270 mm of microorganisms by use of a 100 × microscope objective, (a) oscillatoria bacteria, (b) diatom alga.

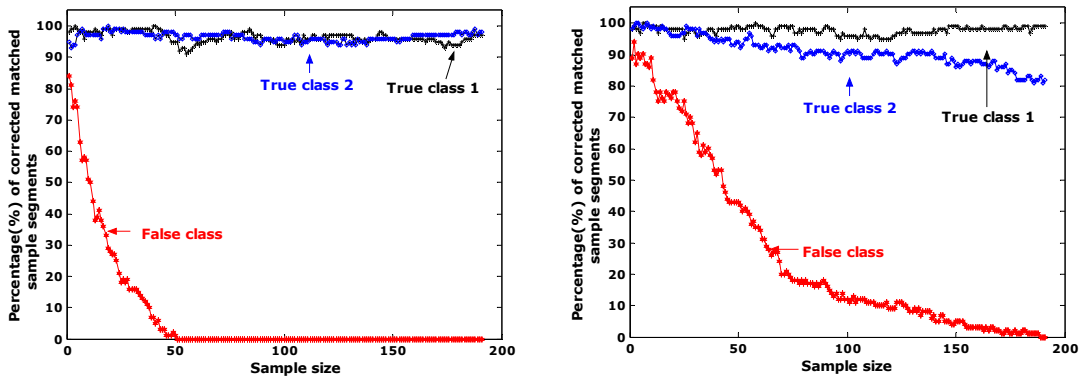

(a) (b)

Fig. 9. (a) Statistical (a) T-test and (b) F-test for checking the equality of the means and the variances between two populations, respectively. True class 1 and 2 : oscillatoria bacteria, false class : diatom alga.

Fig. 9(a) shows the results of the *student's t-test* for the difference of location parameter between the reference and input sample data, where we rejected the null hypothesis $\mathbf{H_0}(\mu_x = \mu_y)$ in case that the statistic T defined in Eq. (11) was outside the range $-t_{0.995} \le T \le t_{0.995}$ on the basis of a two-tailed test at level of significance 0.01. It is noted that the percentages of the correct matched sample data by the decision rule for the true-class1, 2 were over around 95%, while for the false-class the percentages rapidly decreased as a sample size increases.

Fig. 9(b) show experimental results of the percentage (%) of correct matched sample data by the *F-test* for the equality of the variances between the reference and input sample data versus the sample size, where two univariate random sample data (real and imaginary parts in the reconstructed image) separately have been tested. For a statistical decision, we rejected the null hypothesis $\mathbf{H_0}(\sigma_x^2 = \sigma_y^2 = \sigma^2)$ in case that the statistic F defined in Eq. (9) was outside the range $F_{0.005}$ and $F_{0.995}$ on the basis of a two-tailed test at level of significance 0.01. It is noted that the percentage of the correct matched sample data by the decision rule for the true-class1 was over 95%, and for the true-class2 was over 80%, while for the false-class the percentage rapidly decreased as a sample size increases, where we used same specimen as the reference for the true-class1 and different specimen for the true class 2.

6. CONCLUSION

Automatic recognition of biological microorganisms is very challenging because of their dynamic nature such as moving, growing, and varying in size and shape. There are broad applications of real time 3D surveillance and identification of dynamic microscopic bio-organic events. 3D sensing and reconstruction by means of SEOL holographic microscopy is suitable for inspection of dynamic biological microscopic events. The sensing is robust to dynamic movement of microscopic objects and environmental conditions as compared with the multiple-exposure phase-shifting digital holography. The set-up is simpler than off-axis holography and more robust to object size and scale variations. A number of approaches are presented for the recognition of the biological microorganisms. Segmentation extracts regions of interest for further processing. A number of techniques are presented for segmentation of biological microorganisms sensed by SEOL holographic microscopy. In particular, bivariate jointly distributed region snake is developed as a statistical segmentation method maximizing the conditional probability of the target hypothesis assuming a joint Gaussian distribution for the complex pixel amplitude. Shape-tolerant 3D recognition of microorganisms using the statistical cost functions and inference is presented. A number of sampling segments are randomly extracted from the microorganism and processed with cost functions and statistical inference theory. By investigating the Gaussian property of the holographically reconstructed images of microorganisms, we are able to distinguish the sampling segments of the true class object in the database from the different classes of microorganisms presented at the input.

Acknowledgements

This work has been supported by Defense Advanced Research Projects Agency (DARPA).

REFERENCES

1. B. Javidi, I. Moon, S. Yeom, and E. Carapezza, "Three-dimensional imaging and recognition of microorganism using single-exposure on-line (SEOL) digital holography," Opt. Exp. vol. 13, 4492-4506 (2005).
2. I. Moon and B. Javidi, "shape-tolerant three-dimensional recognition of microorganisms using digital holography," Opt. Exp. vol. 13, 9612-9622 (2005).
3. B. Javidi, I. Moon, and S. Yeom, "Real time 3D sensing and identification of microorganism," Optics and Photonics News Magazine vol. 17, 16-21 (2006).
4. B. Javidi, S. Yeom, I. Moon, and M. Daneshpanah, "Real-time automated 3D sensing, detection, and recognition of dynamic biological micro-organic events," Opt. Exp. vol. 14, 3806-3829 (2006).